EUROfusion

WPS1-CPR(17) 17815

P Drews et al.

Topology effects on the edge heat and particle transport in the limiter plasma on W7-X

Preprint of Paper to be submitted for publication in Proceeding of
643. WE Heraeus-Seminar

This work has been carried out within the framework of the EUROfusion Consortium and has received funding from the Euratom research and training programme 2014-2018 under grant agreement No 633053. The views and opinions expressed herein do not necessarily reflect those of the European Commission.

This document is intended for publication in the open literature. It is made available on the clear understanding that it may not be further circulated and extracts or references may not be published prior to publication of the original when applicable, or without the consent of the Publications Officer, EUROfusion Programme Management Unit, Culham Science Centre, Abingdon, Oxon, OX14 3DB, UK or e-mail Publications.Officer@euro-fusion.org

Enquiries about Copyright and reproduction should be addressed to the Publications Officer, EUROfusion Programme Management Unit, Culham Science Centre, Abingdon, Oxon, OX14 3DB, UK or e-mail Publications.Officer@euro-fusion.org

The contents of this preprint and all other EUROfusion Preprints, Reports and Conference Papers are available to view online free at http://www.euro-fusionscipub.org. This site has full search facilities and e-mail alert options. In the JET specific papers the diagrams contained within the PDFs on this site are hyperlinked

Topology effects on the edge heat transport in the limiter plasma on W7-X

P. Drews[1], H. Niemann[2], J. Coesfeld[1], A. Charl[1], Y. Gao[1], J. Geiger[2], O.Grulke[2], M. Henkel[1], D. Höschen[1], K. Hollfeld[3], C. Killer[2], A. Krämer-Flecken[1], Y. Liang[1], S. Liu[1], D. Nicolai[1], O. Neubauer[1], M. Rack[1], N. Wang[4], B. Schweer[1], P. Denner[1], G. Satheeswaran[1], L. Rudischhauser[2], N. Sandri[1] and the W7-X Team[2]

[1]Forschungszentrum Jülich GmbH, Institut für Energie- und Klimaforschung Plasmaphysik, Partner of the Trilateral Euregio Cluster (TEC), 52425 Jülich, Germany

[2]Max-Planck-Institut für Plasmaphysik, Greifswald, Germany

[3]Forschungszentrum Jülich GmbH, Central Institute for Engineering, Electronics and Analytics/Engineering and Technology (ZEA-1), 52425 Jülich, Germany

[4]School of Electrical and Electronic Engineering, Huazhong University of Science and Technology, Wuhan 430074, China

Abstract

Controlling the heat and particle fluxes in the plasma edge and on the plasma facing components is important for the safe and effective operation of every magnetically confined fusion device. This was attempted on Wendelstein 7-X (W7-X) in the first operational campaign, with the modification of the magnetic topology by use of the trim coils and tuning the field coil currents, commonly named iota scan. Ideally, the heat loads on the five limiters are equal. However, they differ between each limiter and are non-uniform, due to the (relatively small) error fields caused by the misalignment of the limiters or intrinsic error fields. It is therefore necessary to study the influence of topology changes on the transport of heat and particles in the plasma edge caused by the application of error fields and the change of the magnetic configuration. In this paper the up-stream measurements conducted with the combined probe are compared to the downstream measurements with the DIAS infrared camera on the limiter.

Keywords: Wendelstein 7-X, plasma edge, heat flux, limiter, multi-purpose manipulator

1 Introduction

The limiter configuration of the first operational campaign of Wendelstein 7-X (W7-X) featured a five-fold symmetric limiter configuration. Ideally, those limiters would experience the same heat loads, but due to an intrinsic error field a considerable asymmetry between the modules was observed [1] [2]. In conjunction with the multi-purpose manipulator, the combined probe has been installed [3] [4], with it measurements of the electron temperature and density have been carried out on W7-X in the first experimental campaign. The electron temperature and density profiles obtained by these measurements [5] are used to calculate the radial heat flux profiles. The influence of the magnetic topology on the radial transport of heat and particles can therefore be studied in respect to the modification of the magnetic topology of the iota scan. These up-stream profiles of the measured temperature, density and the corresponding calculated heat and particle fluxes, can be compared to the downstream measurements of the heat and particle fluxes on the corresponding limiters measured with the DIAS camera [6] and the modelling from EMC3-EIRENE [7][8]. The comparison with the modelling in [8] shows that the measured and modelled electron temperature and density profiles are in good agreement. Hence, the ion temperature profile from the modelling will be used in the following calculations, since the diagnostic coverage of the ion temperature in the plasma edge was still poor in the first operational phase . A direct calculation of the heat fluxes on the limiter was conducted in [9]. Figure 1 shows the position of the manipulator in the mid-plane of module 4 and the field of view of the DIAS camera in module 5. This presents an opportunity to compare the two edge plasma diagnostics.

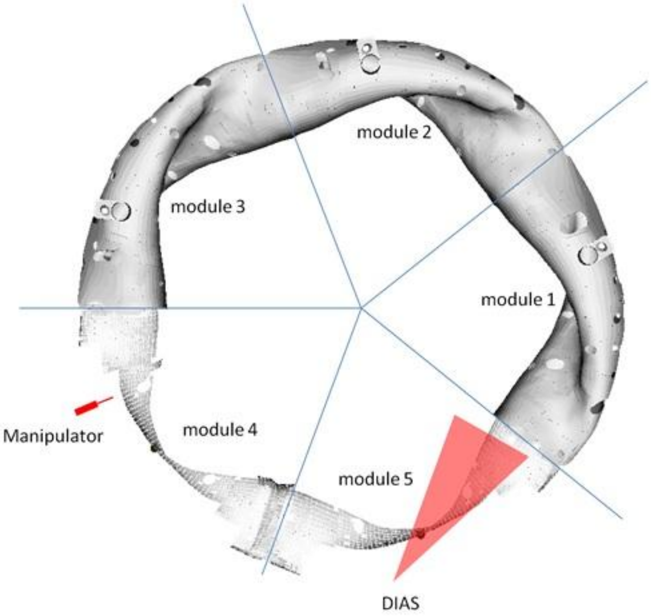

Figure 1. Position of the manipulator in module 4 and of DIAS camera in Module 5

2 Experimental setup

The multi-purpose manipulator (MPM), position indicated in figure 1, was installed on the outboard side of the vacuum vessel on W7-X in 2015 and commissioned in early February 2016 [2] [3]. The manipulator allows both measurements in a static position to observe fluctuation and a fast movement for obtaining profiles. It is located in the mid-plane of module four at the AEK40 flange at the toroidal position ($\varphi = 200.7°$) . It is able to plunge $35\ cm$ into the vacuum vessel. The first diagnostic to be used was the so-called combined probe, which includes among other diagnostics five Langmuir probe pins [10] used in a triple probe configuration.

For the down-stream measurements the DIAS camera was used. The DIAS camera is a micro-bolometer with 8-14μm wave length range, 50 Hz time and about 5 mm spatial resolution. The THEODOR code [11] was used to calculate the heat flux on the limiters based on measured temperatures. The resulting heat flux values has an estimated error of about 0.2 MW/m^2.

The measurements conducted as part of the iota scan will be discussed in the following. The rotational transform was scanned by tuning the planar coils A and according to table 1.

Scenario #	Index	$I_{A\,coil}$ (A)	$I_{B\,coil}$ (A)
20160309013	J configuration	4824	4824
20160309032	Iota index 13	4844	0

Table 1 overview of the discharge number, configurations and coil currents used in the comparison

It is expected that the higher iota configurations experience an inwards shift of the $5/6$ island chain located past the last closed flux surface, while the $5/5$ island moves closer towards the last closed flux surface from the scrape off layer. It is not possible for the probe to measure the $5/6$ island chain directly and the $5/5$ island chain is supposed to be cut off by the limiter.

In figure 2 the two profiles of the electron temperature and density are shown for the J and the higher iota configuration, one can see that the shift of the magnetic axis. The $5/5$ island is also visible for the higher iota case. The measurements were performed at the same ECRH heating of 2 MW.

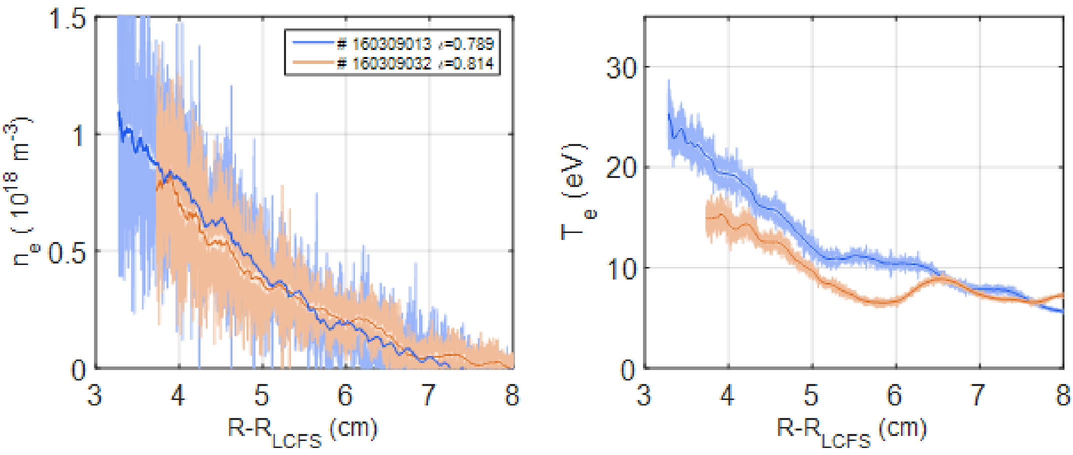

Figure 2 Shift of the electron temperature and density profiles for the J and iota index 13 configuration

3 Mapping of the manipulator on the limiters

The manipulator measurements were conducted in the mid-plane of module 4, while the DIAS camera is monitoring the left side of the limiter in module 5. As mentioned, due to error fields present in the machine an asymmetry of the heat load distribution was observed with thermo-couples on the limiters [1].

One can deduce from [1] that limiter 1 experienced the highest heat flux and limiter 3 the lowest, while the limiters 2, 4 and 5 can be assumed to have similar heat fluxes. The field line tracing web tool supplied by the Max Planck institute [12] was used to trace the field lines from the position of the combined probe to the corresponding wall elements. It is found that the combined probe connects to limiter 1 and 2. For the comparison of the heat fluxes it is assumed that limiter 2 and 5 experience similar heat loads. Therefore, the footprint of the probe on limiter 2 could be projected on limiter 5. In this way the up-stream heat flux calculated from the combined probe data can be mapped on the existing limiter measurements.

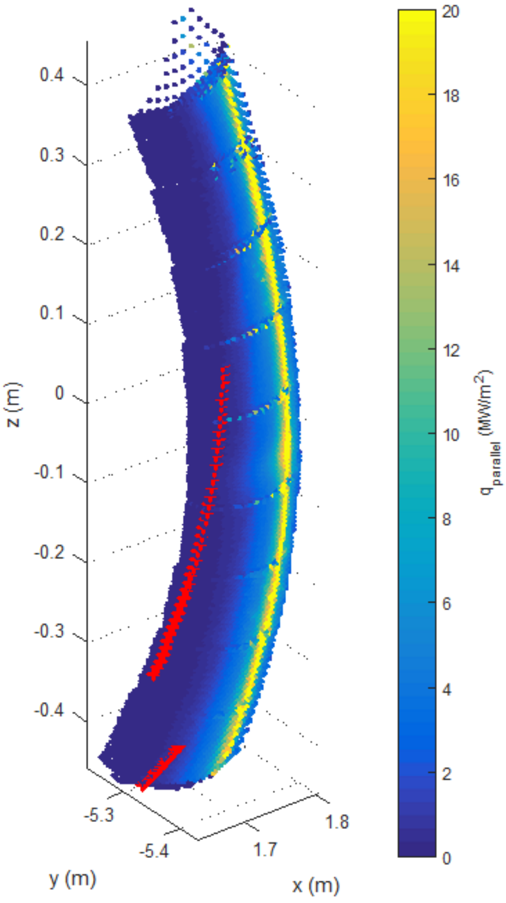

Figure 3 heat flux on limiter 5 measured with the DIAS camera, with the footprint of the combined probe in red crosses

Figure 3 shows the down-stream heat fluxes measured by the DIAS camera and the probe's footprint. The down-stream heat fluxes had to be converted by taking the incidence angle of the field lines into account [9]:

$$q_{||} = \frac{\mathrm{q_{limiter}}}{\sin(\alpha)},$$

with α as the incidence angle of the field lines on the limiter and $\mathrm{q_{limiter}}$ as the heat flux measured with the DIAS camera. The up-stream heat flux profile is calculated using the electron density and temperature profile and the resulting ion sound speed. In addition the ion temperature from the EMC3-EIRENE modelling, shown in figure 4 is used for:

$$q_{probe} = n_e c_s (T_e + T_i),$$

with n_e as the electron density, while assuming quasi neutrality and c_s as the ion sound speed. The considerably higher ion temperature in the edge has to be taken into account to attain a realistic heat flux profile for the up-stream measurements.

Thereby it is possible to compare the parallel heat fluxes. The footprint of the combined probe for limiter 1 is on the side of the limiter that is outside of the DIAS camera's field of view, therefore the comparison in this paper is done for the measurements of limiter 2 and 5.

In the following the projection of limiter 2 on limiter 5 will be called the forward direction of the field line tracing and the projection of limiter 1 on limiter 5 the backward direction.

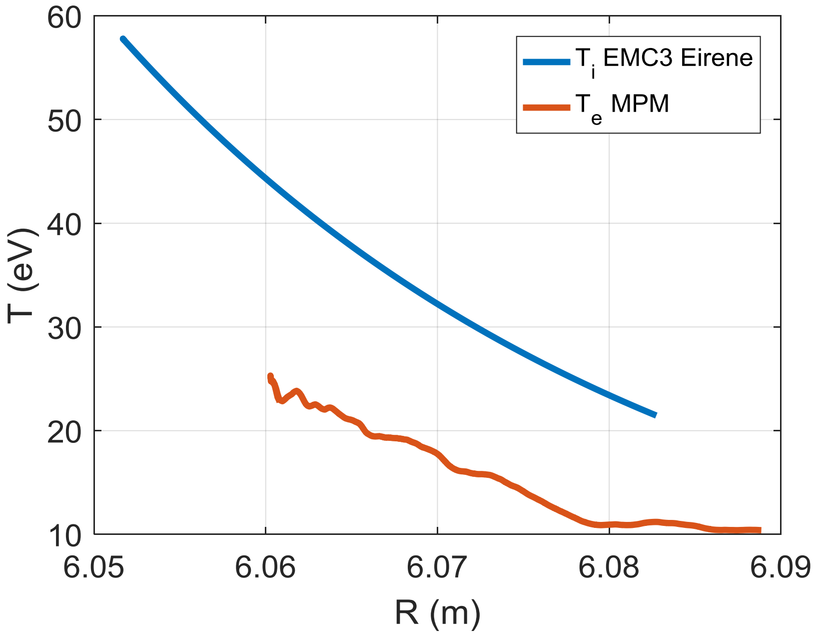

Figure 4 electron temperature measured with the combined probe and ion temperature simulated with EMC3 EIRENE modelling

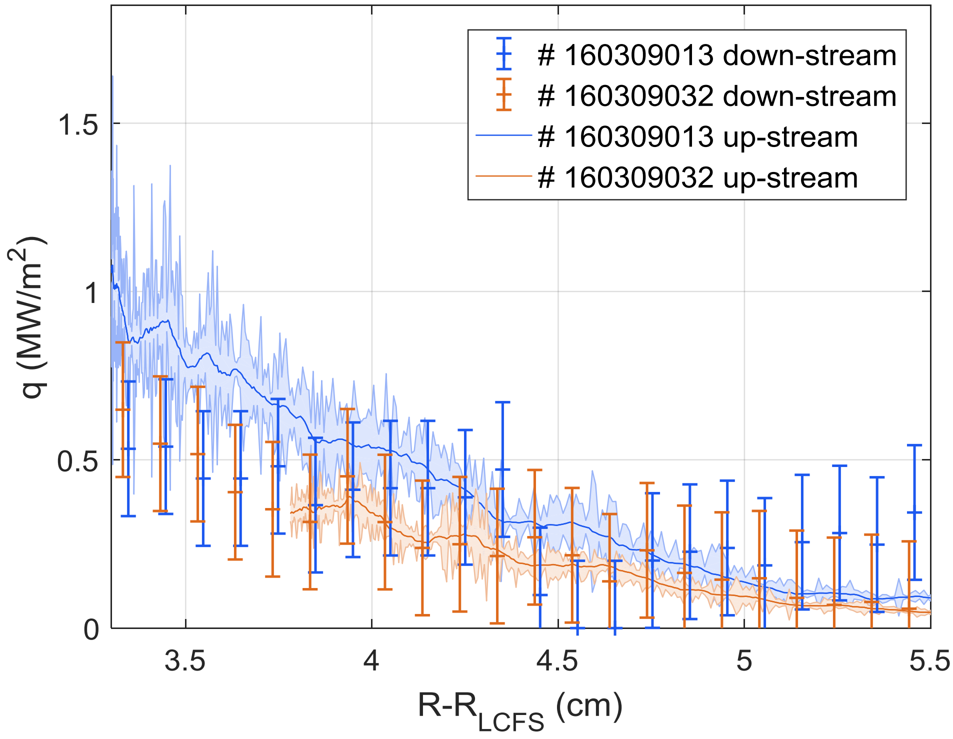

Figure 5 comparison of the heat flux form the combined probe (up-stream) and the DIAS camera (down-stream)

It should be noted here that the measurement for this configuration was conducted in the far scrape off layer where the errors of both measurements are quite large. One can see that the down-stream measurements do not change considerably with the iota scan, the up-stream values on the other hand do. It should be noted that as part of the iota scan the magnetic axis was shifted inwards for higher iota configurations as shown in figure 5. For the J-configuration the up-stream values are larger than the downstream measurements, for the higher iota case both heat flux are comparable within the errors. The measurements with the combined probe were conducted in the far scrape off layer only for technical reasons. More interesting results are expected in the next operation phase where the probe plunges deeper into the plasma. The modelling from EMC3-EIRENE, using the combined probes measurements as input data, can supply also the heat fluxes at any given position in the device. When radiative and other effects are taken into account, the calculation is computationally costly. Using the mapping of the field lines to directly compare the two diagnostics in two different positions represents a fast, although incomplete alternative, as it does not take additional effects like radiative losses into account.

4 Effect of the iota scan on the heat flux distribution

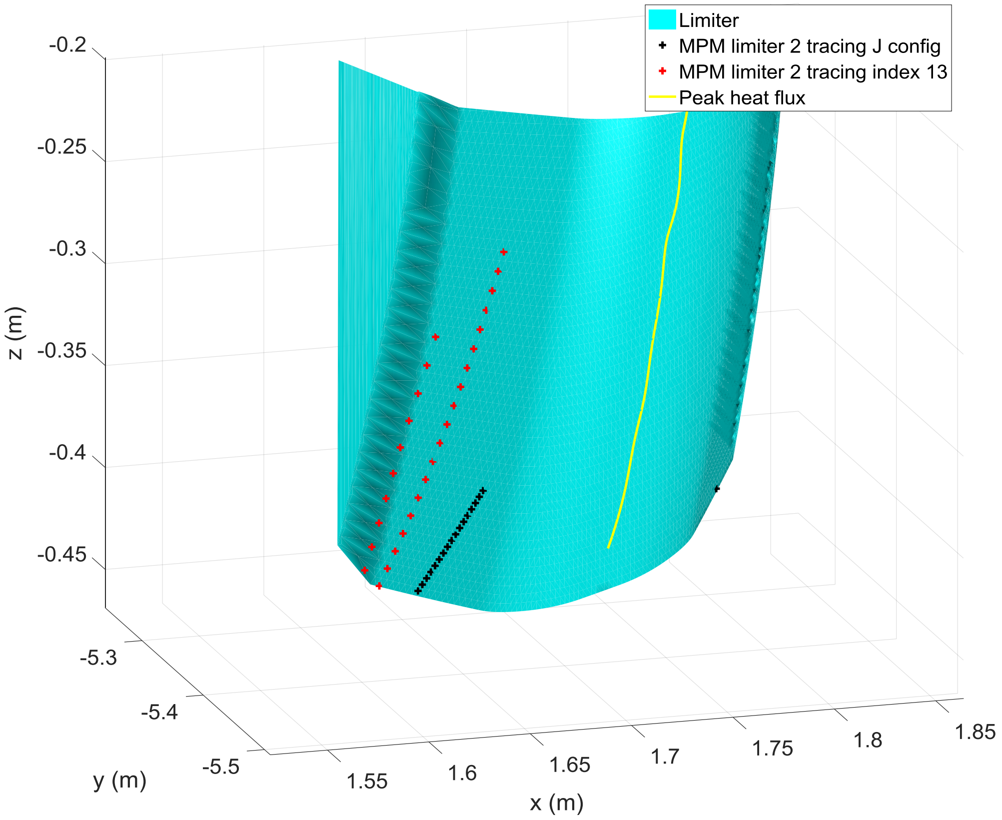

Figure 6 shift of the footprint of the combined probe mapped on the limiter in forward direction, black: limiter J-configuration, red: iota 13 configuration

In figure 6 the footprint in the forward direction is shown for the limiter J-configuration and for the iota index 13 configuration. One can see that while the pattern changes from a single line to two fingers, the distance to the area of the highest heat flux, indicated by the yellow line, does not change significantly. Therefore, the down-stream heat loads do not change for the two different configurations. Figure 7 shows the footprint in the backward direction, here again the single line is branched off into two fingers, but the distance to the strike line increases and thereby the range of the probe experiences a decreased up-stream heat flux.

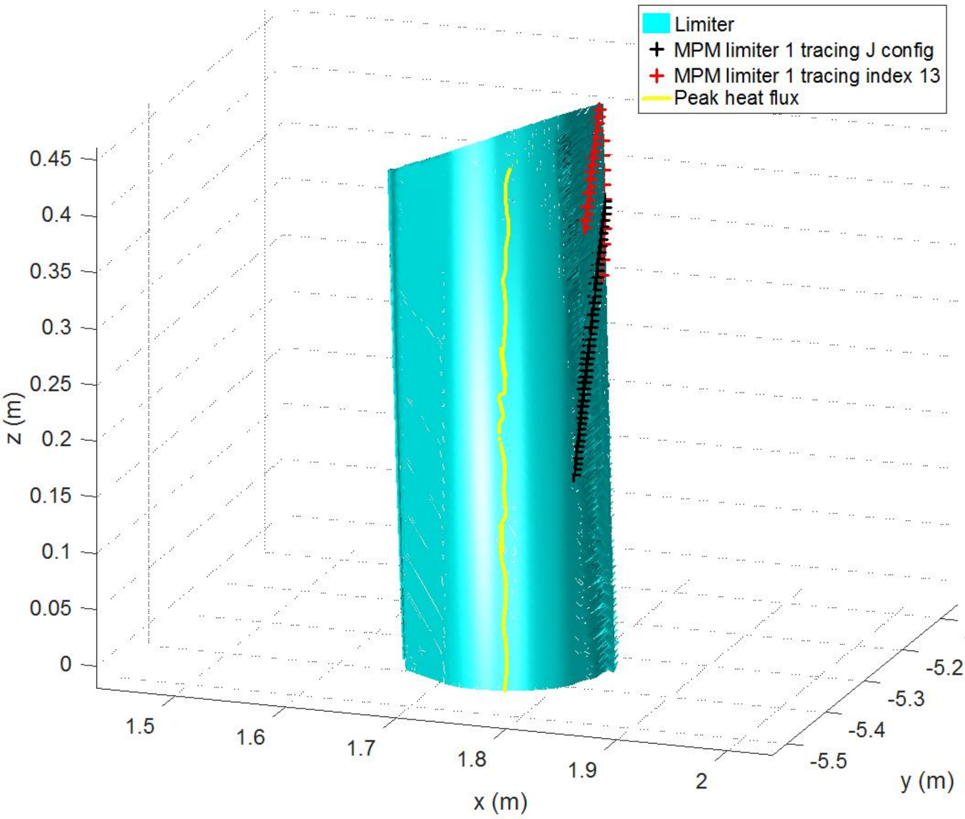

Figure 7 shift of the footprint of the combined probe mapped on the limiter in backward direction, black: limiter J-configuration, red: iota 13 configuration

5 Discussion and conclusion

Mapping the position of the combined probe to the limiters, assuming similar heat loads between certain limiters, allowed for a comparison of the up and down-stream heat fluxes. This comparison showed that the up-stream heat fluxes are as expected higher than the down-stream measurements on the limiter. This is found for the J-configuration and within the error range for the iota index 13 configuration. For a more complete analysis it is necessary to take additional effects like radiative and frictional losses into account. Also it became apparent that additional data on the ion temperature is necessary to get a reasonable estimate for the up-stream heat fluxes. Data supplied from EMC3-EIRENE showed that the ion temperature in the edge is about a factor of two bigger than the electron temperature, which constitutes a huge contribution to the estimated overall heat flux. The iota scan and said mapping show how the heat fluxes on limiter 1 are reduced while the corresponding heat flux on limiter 2 remains largely unchanged with increasing iota. For the second operational campaign an upgrade for the combined probe is planned, which will feature an ion sensitive probe, to simultaneously measure the ion temperature in addition to the Langmuir probes measurements for the electron temperature.

Acknowledgments

This work has been carried out within the framework of the EUROfusion Consortium and has received funding from the Euratom research and training program 2014-2018 under grant agreement No 633053. The views and opinions expressed herein do not necessarily reflect those of the European Commission.

References

[1] G.A. Wurden et al 2017 Nucl. Fusion **57** 056036
[2] S. Bozhenkov et. al, 2017 accepted Nucl. Fusion
[3] D. Nicolai et al 2017 Fusion Eng. Des.
http://dx.doi.org/10.1016/j.fusengdes.2017.03.013
[4] G. Satheeswaran et al., Fusion Eng. Des. (2017),
https://doi.org/10.1016/j.fusengdes.2017.05.125
[5] P. Drews et al 2017 Nucl. Fusion 101605.R3
[6] H. Niemann et al 2016 43rd EPS Conf. on Plasma Physics P4.005
(http://ocs.ciemat.es/EPS2016PAP/pdf/P4.005.pdf)
[7] M. Rack et al 2017 Nucl. Fusion **57** 056011
[8] J. Coesfeld et al 2017 in this journal
[9] F. Effenberg et. al, 2017 Nucl. Fusion **57** 036021
[10] Tonks and Langmuir 1929 Phys Rev. **34** 876-922
[11] A. Hermann et. al and ASDEX Upgrade Team, EPS Vol 25A, 25A (2001)
[12] S. Bozhenkov 2013 Fusion Engineering and Design **88** 2997– 3006